Pap	er	#1	5	05	8
-----	----	----	---	----	---

Poly(butadiene-graft-pentafluorostyrene) as a Coupling Agent in Rubber Compounding

Nicole Swanson,*^a Dr. Kushal Bahl,^b Prasad Raut,^b Dr. Sadhan C. Jana,^b Dr. Coleen Pugh^a

The University of Akron

^aDepartment of Polymer Science

^bDepartment of Polymer Engineering

Akron, Ohio U.S.A.

Presented at the 12th Annual Student Colloquium & Poster Session at the Fall 188th Technical Meeting of the Rubber Division, ACS Cleveland, Ohio U.S.A.

October 14, 2015

ISSN: 1547-1977

^{*}Speaker

ABSTRACT

Reinforcing fillers are necessary in rubber compounding to aid in enhancing the mechanical properties of the compound for various applications. Carbon black (CB) is currently the most common reinforcing filler used in tire compounding. Lignin, an amorphous polyphenolic material derived from plants and a by-product of the pulp and paper industry, is also an attractive material that can serve as a dispersant and as a reinforcing filler. This paper evaluates the interactions between styrene-butadiene rubber and reinforcing fillers with an electron-rich π -system, such as lignin and CB, in the presence of a graft copolymer (PB-g-PPFS) of PB and electron-deficient 2,3,4,5,6-pentafluorostyrene (PFS). The interactions are attributed to areneperfluoroarene interactions between the electron-deficient π -system of the polyperfluoroarene grafts and the electron-rich π -system of lignin and/or CB particles. The effects of improved filler-rubber interactions on mechanical properties and dynamic mechanical properties are analyzed. This paper will demonstrate the use of PB-g-PPFS as a coupling agent in rubber compounds to enhance the interaction between the filler, lignin and lignin-carbon black hybrid filler, and the rubber matrix to achieve a reduction in the hysteresis loss and enhanced filler dispersion.

1. INTRODUCTION

Coupling agents in rubber compounding provide a bridge between the rubber matrix and the filler network to enhance the mechanical properties of the compound. This interaction between the rubber matrix and filler network may be covalent or non-covalent. One well studied, non-covalent, intermolecular interaction is the arene-perfluoroarene interaction or π - π stacking between electron-rich and electron-deficient π -systems. Patrick and Prosser first documented crystal formation (m.p. = 24 °C) from a 1:1 mixture of benzene (m.p. = 5.5 °C) and hexafluorobenzne (m.p. = 5 °C). The increased melting point of the resulting crystal indicated that a complex formed by arene-perfluoroarene interactions between the electron-rich benzene π -system and electron-deficient hexafluorobenzene π -system. By utilizing the concept of arene-perfluoroarene interactions, a polybutadiene graft copolymer containing pendant electron-deficient pentafluorostyrene grafts (PB-g-PPFS) was synthesized to be used as a coupling agent in rubber compounding, Which is the focus of this paper.

Lignin is a natural, organic polymer that originates as a component of vascular plants and is a by-product of the pulp and paper industry. Second to cellulose in natural abundance, the chemical structure of lignin consists of substituted benzene rings with alkyl, alkoxy and hydroxyl substituents. This renders lignin's aromatic π -system relatively electron-rich. The particular delignification method used to extract lignin from the tree pulp is what determines the chemical structure. Kraft lignins are more electron-rich than lignosulfonates from the sulfite pulping method. Due to the presence of the alkoxy and hydroxyl substituents on kraft lignin, it becomes incompatible with non-polar polymers such as rubber. Therefore, chemical modification of the lignin, 22–24 the formation of a hybrid filler and the use of coupling agents to improve the compatibility of lignin with rubber have been studied.

The focus of this paper is to demonstrate the use of PB-g-PPFS as a coupling agent utilizing arene-perfluoroarene interactions to enhance the kraft lignin and lignin-carbon black hybrid filler dispersions in the rubber network to reduce the hysteresis loss and improve mechanical properties and filler dispersion.

2. EXPERIMENTAL

2.1 Synthesis of Poly(butadiene-*graft*-pentafluorostyrene)

Following a previously reported procedure (Scheme 1),^{15,26} the PB-*g*-PPFS was synthesized using a 2:1 molar ratio of PFS and PB. The crude polymer was a mixture of PB-*g*-PPFS graft copolymer, PPFS homopolymer and up to a trace amount of unreacted PB and was used as the coupling agent in SBR compounds with kraft lignin and kraft lignin-carbon black (KL-CB) hybrid particles as the fillers.

The PB-g-PPFS graft copolymer was characterized by 1 H (300 MHz) and 19 F (297 MHz) NMR spectroscopy (δ , ppm) on the Varian Mercury 300 spectrometer recorded in CDCl₃ and referenced to residual solvent and trifluoroacetic acid for 19 F NMR. The molecular weight was characterized by gel permeation chromatography (GPC_{PSt}) relative to linear polystyrene standards at 35 $^{\circ}$ C using THF as the solvent at a flow rate of 1.0 mL/min with a guard column and a set of 50, 100, 500 and 10^4 Å and linear (50- 10^4 Å) Styragel columns equipped with a Waters 410 differential refractometer (RI) and a Waters 486 tunable UV/Vis detector set at 254 nm and Millennium Empower 3 software. Graft copolymer parameters (i.e. monomer conversion, grafting efficiency, graft ratio and frequency) were calculated from the GPC trace of the crude

graft copolymer following previously reported methods.²⁶ Table 1 shows the graft copolymer values obtained from GPC characterization.

2.2 Styrene-Butadiene Rubber (SBR) Compound Preparation

Prior to compounding, the coupling agent, PB-g-PPFS, and the kraft lignin powder were mixed in THF to promote the formation of interactions between the electron-rich KL π -system and the electron-deficient PFS π -system of PB-g-PPFS. The same procedure was used with the KL-CB hybrid fillers. The PB-g-PPFS coupling agent was dissolved in THF and the kraft lignin filler, or KL-CB hybrid filler, was added and stirred until all THF had evaporated. Table 2 summarizes the amounts of the lignin fillers and coupling agent used in the rubber compounds.

The compounds of SBR with KL and KL-CB hybrids with and without the coupling agent were mixed in two steps in a Brabender Plasticorder internal mixer (80 cm 3 volume). The first step involved mixing the SBR, zinc oxide, stearic acid and filler, treated or non-treated depending on the batch, at a rotor speed of 65 rpm and a fill factor of 0.7 at 80 °C. The rubber was masticated for 60 s and mixed with the remaining ingredients for 5 min. The second step involved mixing the rubber compound obtained in step 1 with the sulfur and CBS accelerator on the two-roll mill for 5-7 min at a speed of 15 rpm with a roll temperature of 40 °C. The mixtures were cured on a compression molder at 160 °C using the optimum curing time (t_{95}), the time needed to reach 95% of the maximum torque. The cured sheet mold samples were used for evaluation of the filler dispersion and reinforcement behavior.

2.3 Characterization Methods

To characterize the arene-perfluoroarene interactions between kraft lignin and PB-g-PPFS, UV-vis spectroscopy was performed on the Hewlett Packard Model 8453 spectrometer using THF as the solvent and reference. The concentrations used were 0.02 g/L of KL and 0.1 g/L of PB-g-PPFS in THF, respectively.

As previously reported,¹⁵ the cure characteristics, mechanical properties and morphology of the rubber vulcanizates were analyzed. The curing parameters such as scorch time, torque difference, and cure time (t₉₅) were calculated from analysis of 5 g specimens in the Movie Die Rheometer (MDR 2000) at a temperature of 160 °C with a frequency of 1.67 Hz and 7 % strain. Crosslink density was measured from the degree of swelling in toluene. The tensile strength was measured on dumb-bell shaped specimens as per ASTM D412, Type C method standards at room temperature using the Instron® 5567 tensile tester with a crosshead speed of 500 mm/min.

3. Results and Discussion

3.1 PB-g-PPFS Characterization

Following previously reported NMR analysis of PB-g-PPFS by Paz-Pazos and Pugh, 26 the 1 H and 19 F NMR spectra of the crude PB-g-PPFS shows resonances for the PB backbone as well as resonances for PPFS confirm the production of the PB-g-PPFS graft copolymers. The 1 H NMR resonances in Figure 1 correspond to the following protons: C H_2 of PPFS (2.00 ppm), cis-C H_2 -CH= of the PB backbone (2.09 ppm), mr + rr CH of PPFS (2.39 ppm), mm CH of PPFS (2.74 ppm), cis-CH $_2$ -CH= of PB backbone (5.39 ppm) and residual butylated hydroxytoluene (BHT) resonances added during precipitation as an antioxidant and radical inhibitor. The 19 F NMR spectrum, as shown in Figure 2, is referenced to trifluoroacetic acid (TFAA) and contains the C3-F (-164.2 ppm),

C4-**F** (-157.1 ppm) and C2-**F** (-146.0 ppm). Paz-Pazos and Pugh²⁶ had previously isolated the PB-g-PPFS graft copolymer from the PPFS homopolymer and unreacted PB to confirm the presence of the graft copolymer in the crude mixture.

3.2 Arene-Perfluoroarene Interaction Analysis

The arene-perfluoroarene interactions were confirmed using UV-vis spectroscopy analysis between kraft lignin and PB-g-PPFS graft copolymer. Figure 3 represents the UV-vis spectra for KL, PB-g-PPFS, the mixture of KL and PB-g-PPFS, as well as the additive spectrum of the individual KL and PB-q-PPFS spectra in the absence of any intermolecular interactions. The spectrum of the kraft lignin in THF has a representative absorbance at approximately 210 nm, attributed to the substituted aromatic units in lignin, and a second absorbance at around 280 nm attributed to the non-conjugated groups in lignin. These two absorbancies are consistent with previously reported values for isolated lignins.^{27–31} The UV-vis spectrum of PB-g-PPFS in THF shows two absorbancies at approximately 213 nm and ~261 nm. Comparison of the additive spectrum with that of the mixture of KL and PB-g-PPFS in THF (Figure 3) confirms the presence of an intermolecular interaction between the electron-rich KL and electron-deficient PPFS of PBg-PPFS. The intensity of the absorbance at ~210 nm for the mixture is less than that of the additive spectrum despite maintaining identical concentrations. There is a red shift in the mixture spectrum to 222 nm from 210 and 213 nm for the KL and PB-g-PPFS spectra, respectively. This red shift is consistent with π - π stacking due to arene-perfluoroarene interactions between the KL and PB-g-PPFS. There is no shift in the KL absorbance at 280 nm or the PB-g-PPFS

absorbance at 261 nm, which is expected since the 280 nm absorbance represents the non-conjugated groups of KL and are not involved in π - π stacking.

The morphology of the KL particles and KL with PB-*g*-PPFS mixtures was analyzed by scanning electron microscopy (SEM). Figure 4 represents the SEM images of (a) KL milled to particle sizes less than 100 µm, (b) PB-*g*-PPFS precipitated from THF and (c) and (d) KL and PB-*g*-PPFS mixture precipitated from THF at different magnifications. Figure 4 (c) and (d) represents no change in the morphology of the KL particles due to the addition of PB-*g*-PPFS. The surface of the large PB-*g*-PPFS particle shows adherence of KL particles to the surface, which is attributed to the arene-perfluoroarene interactions between the electron-deficient PPFS grafts and electron-rich KL particles. A 90:10 weight ratio of KL:PB-*g*-PPFS was used; therefore, there is an excess of KL particles, as shown in Figure 4 (c) and (d).

3.3 Rubber Compound Analysis

The results of curing the rubber compounds at 160 °C with and without the PB-g-PPFS coupling agent were analyzed on a moving die rheometer. This study showed the effect of the coupling agent on the cure parameters such as the scorch time, cure time and difference in torque (ΔM). The difference in the scorch time and the ΔM values were insignificant when comparing to the compounds with and without coupling agent, as reported previously by Bahl et al. The cure time, as shown in Figure 5, is different for compounds with and without the coupling agent, but the difference is more prominent in the KL compounds than the KL-CB hybrid filler compounds. A decrease in the curing rate in the system containing no coupling agent and only KL as the filler is attributed to large quantities of polar lignin. The polar lignin filler can

interact and react with the curing agents, and thereby increase the cure time. The decrease in cure time when the coupling agent is added (SBR-30KL w/copolymer) is attributed to the arene-perfluoroarene interactions between the KL and PB-g-PPFS coupling agent, which reduces the ability of the lignin to interact with the curing agents. The same argument is true for the KL-CB hybrid filler compounds, but due to the CB present, the difference is not as significant.

The mechanical properties of the SBR compounds containing KL and KL-CB hybrid fillers with and without coupling agent were analyzed. Table 3 shows the values of tensile strength, strain at break, M100 and the apparent crosslink density of these compounds. The tensile strength increased upon the addition of the coupling agent; the increase was approximately 20 % when KL was used as the filler and about 10% when KL-CB hybrid filler was used. The increase in tensile strength with the use of PB-g-PPFS is attributed to the arene-perfluoroarene interactions providing efficient coupling between the KL filler and rubber matrix and enhanced dispersion. The tensile strength of 12.12 MPa for SBR-30KLCB1090 with PB-g-PPFS is comparable to previously reported²⁵ tensile strength for a 30 phr CB filled SBR compound (12.8 ± 1.54 MPa). This comparable tensile strength shows that some kraft lignin can be used to substitute part of the CB filler in the formulation.

The 100% modulus (M100) for the SBR-30KL with PB-g-PPFS slightly increased compared to that without coupling agent, while the strain at break decreased. This slight increase in stiffness may be credited to the increased interaction between KL and the rubber matrix from the use of the coupling agent. The SBR-30KLCB1090 with and without coupling agent had little to no change in the strain at break, M100 and apparent crosslink density. This is because of the

decreased amount of KL in the KL-CB hybrid filler; the ability to utilize arene-perfluoroarene interactions is not as significant as the sample with KL only as the filler.

The dynamical mechanical analysis (DMA) data for the SBR compounds with KL and KL-CB hybrid fillers was analyzed at 60 °C and 1 Hz frequency to analyze the effect of the PB-g-PPFS coupling agent on the rolling resistance indicator (tan δ at 60 °C), as shown in Figure 6. The increased stiffness (M100) of the KL compound with coupling agent is responsible for a lower value of tan δ , or improved rolling resistance, and increase in storage modulus. The addition of the PB-g-PPFS aids in improving the rubber-filler interaction and reducing the filler-filler networking. In the case of the compounds with KL-CB hybrid filler, there is a slight decrease in both the storage modulus and tan δ upon addition of PB-g-PPFS. This is attributed to an improvement in rubber-filler networking and a decrease in the filler-filler network, independent of the stiffness since it did not change nor did the apparent crosslink density for these KL-CB hybrid filler compounds.

The filler dispersion was analyzed using scanning electron microscopy of the fractured surfaces of the SBR KL-CB hybrid filler compounds with and without coupling agent (Figure 7). The hybrid filler domains are outlined in the micrograph; the size of these domains decrease with the addition of PB-g-PPFS. Without the coupling agent, the hybrid filler domain size ranges from 30-50 µm, but with the coupling agent it decreases significantly. The arene-perfluoroarene interactions between the electron-rich KL filler and electron-deficient PPFS of PB-g-PPFS improved the filler dispersion. The filler dispersion analysis is consistent with the DMA data in improving the interaction between the filler and rubber matrix and reducing the filler-filler network.

4. Conclusions

The use of arene-perfluoroarene interactions to establish non-covalent interactions between lignin filler and rubber was successfully demonstrated. The PB-g-PPFS graft copolymer was used as a coupling agent to enhance this interaction between the SBR rubber matrix and polar lignin filler. The PB backbone is compatible with the SBR and the electron-deficient PPFS grafts interact with the electron-rich lignin filler. UV-vis spectroscopy and SEM images confirm interaction between the lignin filler and PPFS grafts of PB-g-PPFS. Upon addition of the PB-g-PPFS coupling agent to the KL-filled SBR, there is an improvement in the failure properties, tensile strength, increased stiffness and reduction in the rolling resistance. All of this is attributed to enhanced filler dispersion due to the coupling between the rubber matrix and filler. The tensile strength increased by 10 % with the addition of PB-g-PPFS for the KL-CB hybrid filler SBR compounds, comparable to the CB filled SBR compounds. 25 The decline in the storage modulus and tan δ at 60 °C for the KL-CB hybrid filler system with PB-g-PPFS is due to improved fillerrubber interactions. The strength of the π - π stacking interactions can be changed by varying the grafting parameters of the PB-g-PPFS. Current studies are looking at that effect with CB filled SBR compounds.

Acknowledgements

This lignin-filled SBR compound work was financially supported by Triangle Tire Company and the current CB-filled SBR compound work is financially supported by CenTiRe.

References

- (1) Hepburn, C. In *Rapra Review Reports*; Rapra Technology Limited, 1997.
- (2) Williams, J. H.; Cockcroft, J. K.; Fitch, A. N. *Angew. Chemie Int. Ed. English* **1992**, *31*, 1655–1657.
- (3) Williams, J. H. Acc. Chem. Res. **1993**, 26, 593–598.
- (4) Hunter, C. A. J. Mol. Biol. **1993**, 230, 1025–1054.
- (5) Cabaco, M. I.; Danten, Y.; Besnard, M.; Guissani, Y.; Guillot, B. *J. Phys. Chem. B* **1998**, *102*, 10712–10723.
- (6) Coates, G. W.; Dunn, A. R.; Henling, L. M.; Ziller, J. W.; Lobkovsky, E. B.; Grubbs, R. H. *J. Am. Chem. Soc.* **1998**, *7863*, 3641–3649.
- (7) Collings, J. C.; Roscoe, K. P.; Robins, E. G.; Batsanov, A. S.; Stimson, L. M.; Howard, J. a. K.; Clark, S. J.; Marder, T. B. *New J. Chem.* **2002**, *26*, 1740–1746.
- (8) Cox, E. G. Rev. Mod. Phys. **1958**, 30, 159–162.
- (9) Dai, C.; Nguyen, P.; Marder, T. B.; Scott, A. J.; Clegg, W.; Viney, C. *Chem. Commun.* **1999**, 2493–2494.
- (10) Feast, W. J.; Lövenich, P. W.; Puschmann, H.; Taliani, C. Chem. Commun. 2001, 505–506.
- (11) Jennings, W. B.; Farrell, B. M.; Malone, J. F. Acc. Chem. Res. 2001, 34, 885–894.
- (12) Knapp, C.; Lork, E.; Mews, R.; Zibarev, A. V. Eur. J. Inorg. Chem. 2004, 2004, 2446–2451.
- (13) Patrick, C. R.; Prosser, G. S. *Nature* **1960**, *187*, 1021–1021.
- (14) Smith, C. E.; Smith, P. S.; Thomas, L.; Robins, E. G.; Collings, J. C.; Dai, C.; Scott, A. J.; Borwick, S.; Batsanov, A. S.; Watt, S. W.; Clark, S. J.; Viney, C.; Howard, J. a K.; Marder, T. B. Synthesis (Stuttg). 2004, 413–420.

- (15) Bahl, K.; Swanson, N.; Pugh, C.; Jana, S. C. *Polymer* **2014**, *55*, 6754–6763.
- (16) Harkin, J. M. Lignin Production and Detection in Wood; 1966.
- (17) Adler, E. Wood Sci. Technol. 1977, 8, 169–218.
- (18) Dimmel, D. In *Lignin and Lignans: Advances in Chemistry*; Heitner, C.; Dimmel, D. R.; Schmidt, J. A., Eds.; CRC Press: Boca Raton, FL, 2010; pp. 18–27.
- (19) Lebo Jr., S. E.; Gargulak, J. D.; McNally, T. J. Lignin. *Kirk-Othmer Encyclopedia of Chemical Technology*, 2002, *3*, 100–124.
- (20) Gierer, J. Wood Sci. Technol. 1985, 19, 289-312.
- (21) Gierer, J. Wood Sci. Technol. **1986**, *20*, 1–33.
- (22) Setua, D. K.; Shukla, M. K.; Nigam, V.; Singh, H.; Mathur, G. N. *Polym. Compos.* **2000**, *21*, 988–995.
- (23) Benko, D. A.; Hahn, B. R.; Cohen, M. P.; Dirk, S. M.; Cicotte, K. N. Functionalized Lignin, Rubber Containing Functionalized Lignin and Products Containing such Rubber Composition. 8,664,305 B2, 2014.
- (24) Bahl, K.; Jana, S. C. J. Appl. Polym. Sci. **2014**, 131, 1–9.
- (25) Bahl, K.; Miyoshi, T.; Jana, S. C. *Polym.* **2014**, *55*, 3825–3835.
- (26) Paz-Pazos, M.; Pugh, C. J. Polym. Sci. Part A Polym. Chem. 2005, 43, 2874–2891.
- (27) Deng, Y.; Feng, X.; Yang, D.; Yi, C.; Qiu, X. BioResources **2012**, 7, 1145–1156.
- (28) Bolker, H.; Somerville, N. *Tappi* **1962**, *45*, 826.
- (29) Todorciuc, T.; Capraru, A.-M.; Kratochvilova, I.; Popa, V. I. *Cellul. Chem. Technol.* **2009**, *43*, 399–408.
- (30) Malutan, T.; Nicu, R.; Popa, V. I. *BioResources* **2008**, *3*, 13–20.
- (31) Pew, J. C. J. Org. Chem. 1963, 28, 1048–1054.

Scheme 1. Synthesis of PB-g-PPFS.

PB-g-PPFS Graft Copolymer M _n x 10 ⁻⁵ (Da)	PB- <i>g</i> -PPFS Graft Copolymer M _w x 10 ⁻⁵ (Da)	PPFS M _n x 10 ⁻⁴ (Da)	Monomer Conversion (%)	Graft Ratio (g/g)	Grafting Efficiency (%)	Graft Frequency
4.85	7.27	1.5	32	0.23	8	1452

Table 1. Molecular weight data and graft parameters for crude PB-g-PPFS determined by GPC_{PSt}.

Material	SBR-OF	SBR-30KL	SBR-30KL w/copolymer	SBR- 30KLCB1090	SBR- 30KLCB1090 w/copolymer
SBR	100	100	100	100	100
Zinc Oxide	3	3	3	3	3
Stearic Acid	1	1	1	1	1
Sulfur	1.75	1.75	1.75	1.75	1.75
CBS	1	1	1	1	1
Lignin	-	30	30	-	-
KLCB 1090	-	-	-	30	30
PB-g-PPFS	-	-	3.3	-	1

Table 2. Rubber compounding formulation for SBR compounds. All amounts are in parts per hundred rubber (phr).

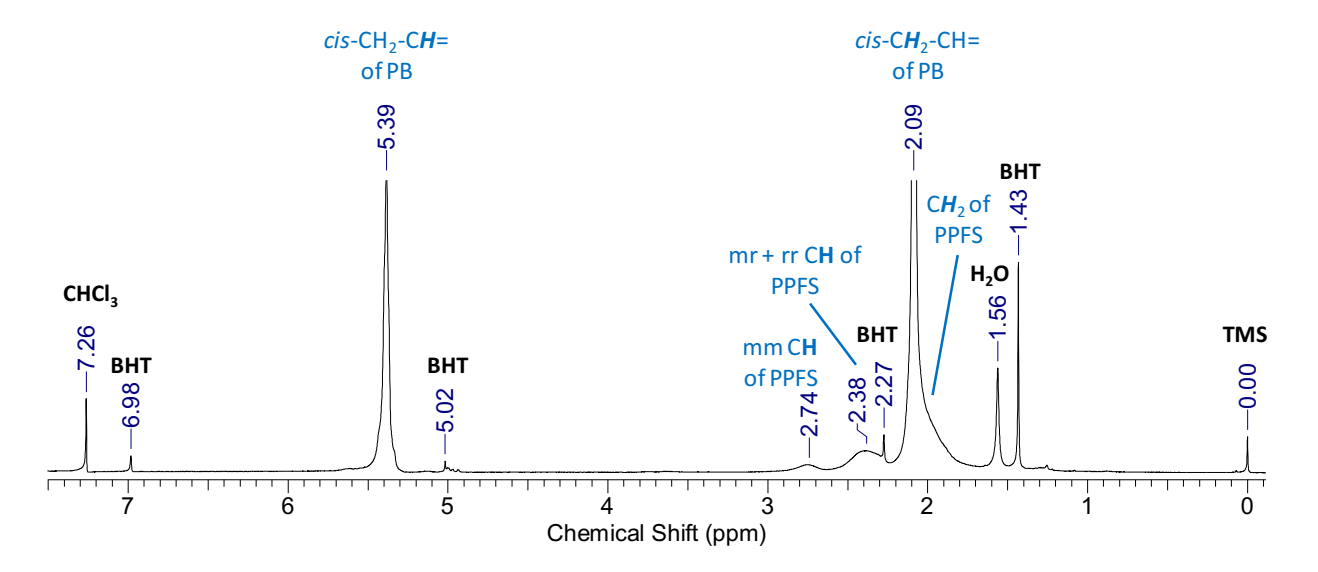


Figure 1. ¹H NMR (300 MHz) spectrum of crude PB-g-PPFS.

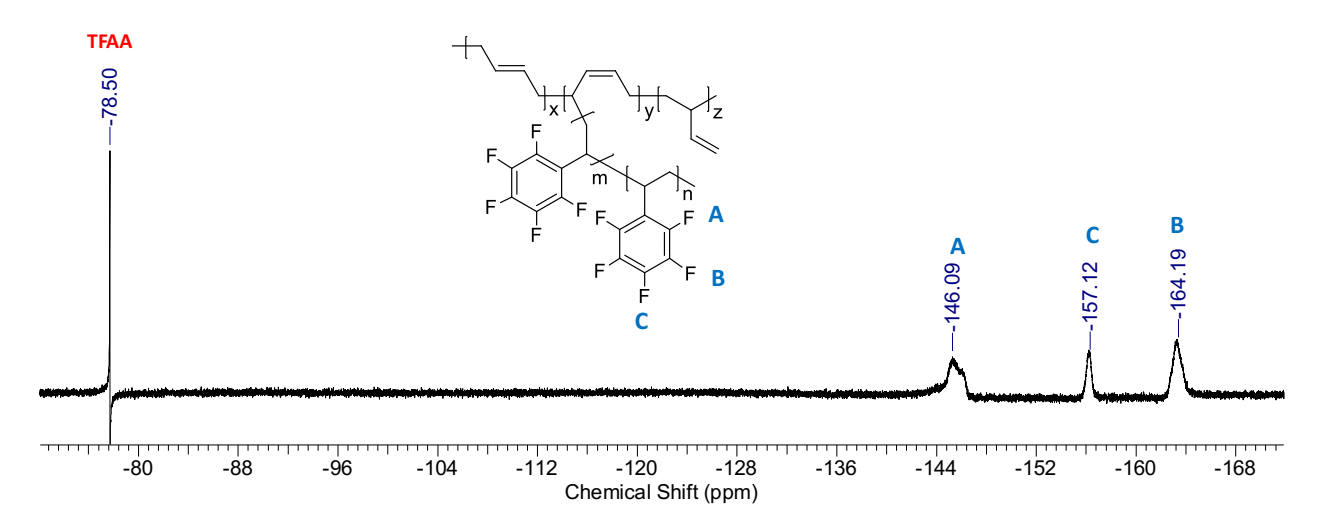


Figure 2. ¹⁹F NMR (297 MHz) spectrum of crude PB-*g*-PPFS.

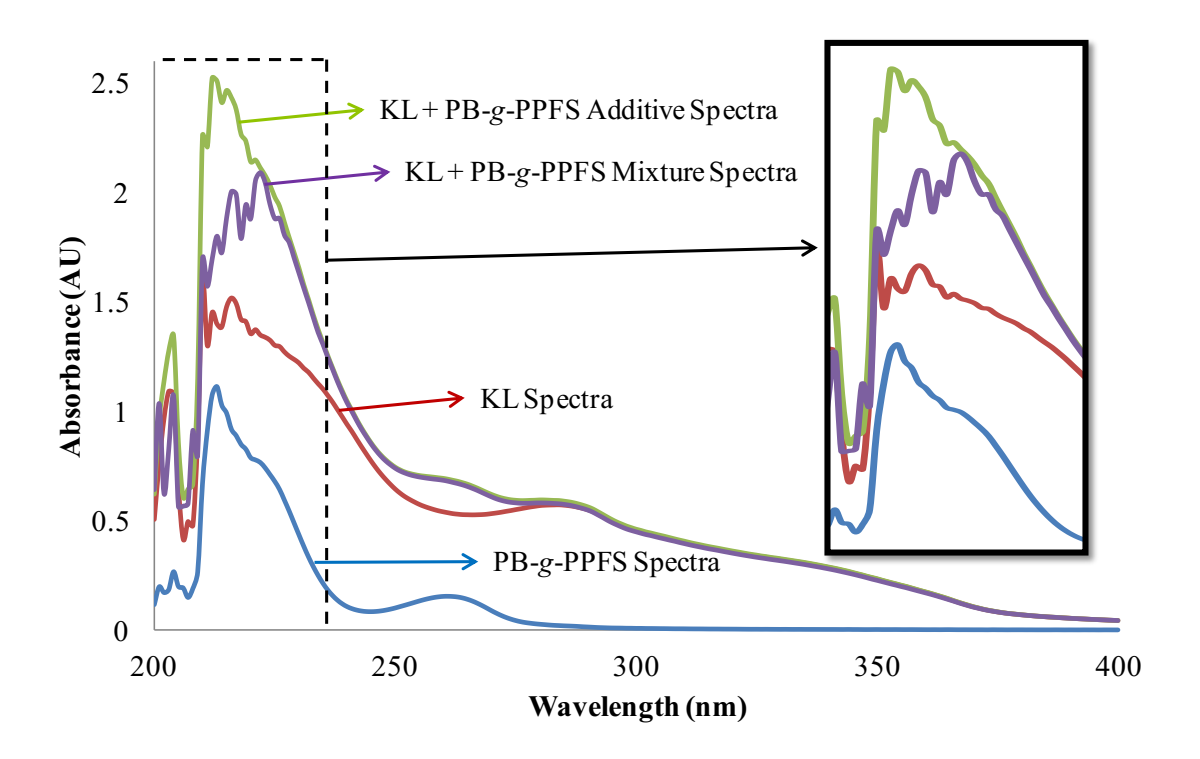


Figure 3. UV-vis spectra of kraft lignin (KL), PB-*g*-PPFS and a mixture of the two in THF. The additive spectrum is the addition of the spectral values for the individual KL and PB-*g*-PPFS spectra. (Reproduced from *Polymer* **2014**, *55*, 6754–6763.)

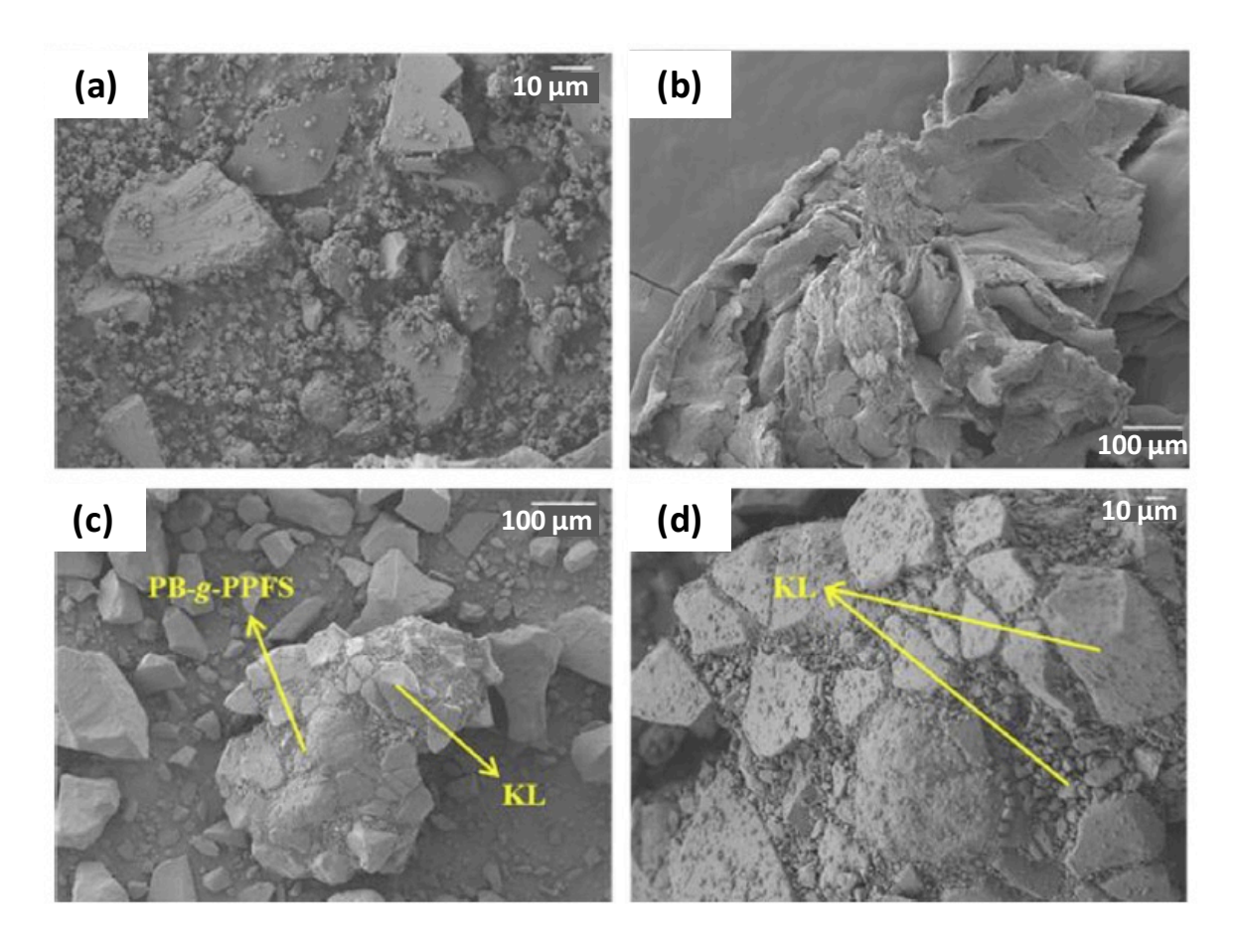


Figure 4. SEM images of (a) KL milled to particle sizes less than 100 μ m, (b) PB-g-PPFS precipitated in THF and (c) and (d) are KL and PB-g-PPFS mixtures at different magnifications. (Reproduced from *Polymer* **2014**, *55*, 6754–6763.)

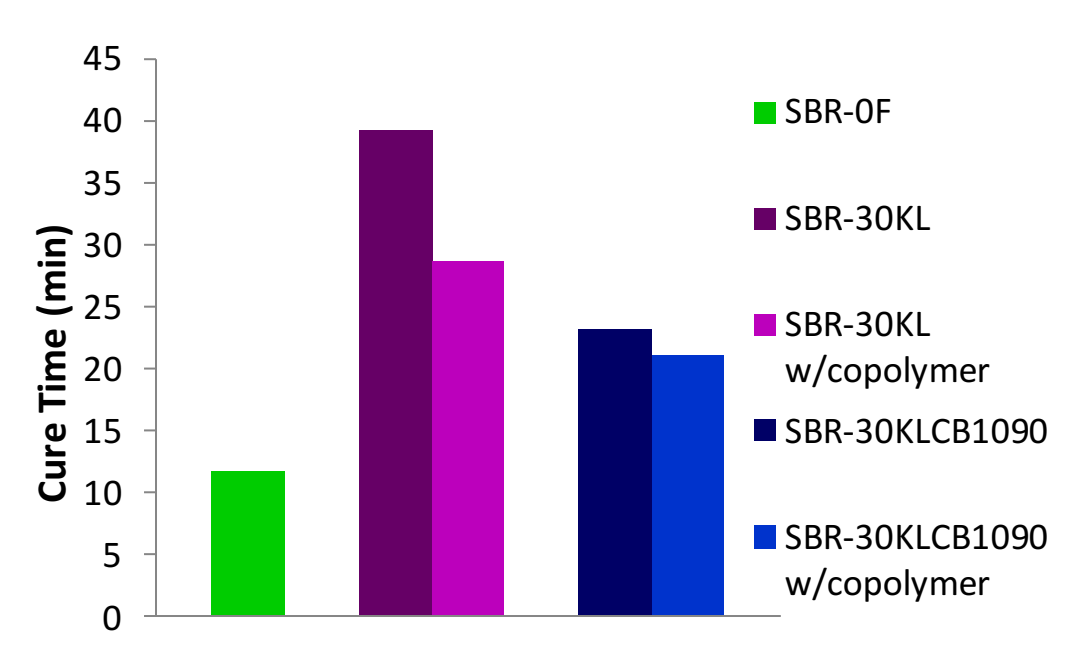


Figure 5. Cure time of SBR compounds with no filler (SBR-0F), 30 phr KL filler (SBR-30KL) and 30 phr 30KLCB1090 hybrid filler (KL:CB 10:90 parts by weight) with and without coupling agent.

Sample	Tensile Strength (MPa)	Strain at Break (%)	M100 (MPa)	(XLD) _{app} (kmol/m³)
SBR-0F (phr)	1.51 ± 0.08	247.2 ± 22.7	1.00 ± 0.02	0.08
SBR-30KL (phr)	1.67 ± 0.14	431.7 ± 57.9	1.14 ± 0.02	0.04
SBR-30KL w/PB-g-PPFS	2.00 ± 0.08	373.7 ± 19.5	1.30 ± 0.03	0.044
SBR-30KLCB1090	11.06 ± 0.78	545.5 ± 30.2	1.88 ± 0.04	0.08
SBR-30KLCB1090 w/PB-g-PPFS	12.12 ± 1.41	556.8 ± 35.3	1.88 ± 0.03	0.08

Table 3. Comparison of the mechanical properties of SBR compounds of KL and KL-CB hybrid fillers with and without coupling agent PB-g-PPFS. (XLD)_{app} is apparent crosslink density.

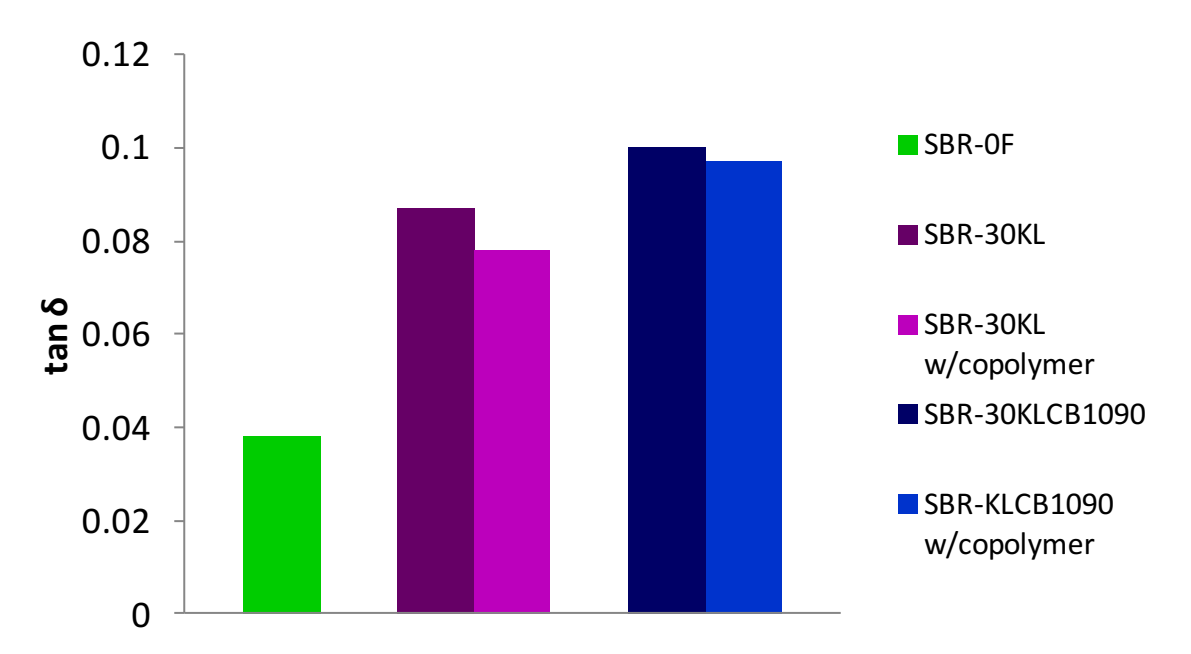


Figure 6. Dynamical mechanical analysis rolling resistance indicator data for SBR compounds of KL and KL-CB hybrid fillers with and without coupling agent.

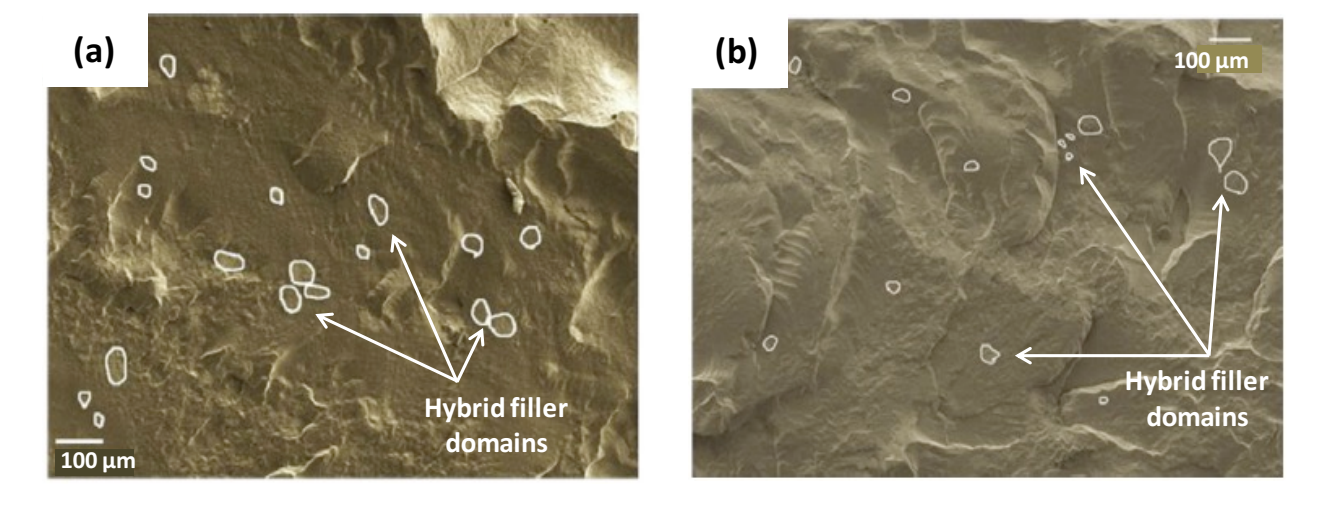


Figure 7. SEM images of fracture surfaces for filler dispersion analysis of KL-CB hybrid filler (a) without and (b) with PB-g-PPFS coupling agent. Hybrid filler domains outlined.